

Preparation and properties of 0.5BiFeO₃–0.5PbFe_{0.5}Nb_{0.5}O₃ ceramics and polycrystalline films

K. M. Zhidel^{*,‡} and A. V. Pavlenko^{*,†}

^{*}Research Institute of Physics, Southern Federal University
No. 194 Stachki Avenue, Rostov-on-Don 344090, Russia

[†]Federal Research Centre
The Southern Scientific Centre of the Russian Academy of Sciences
No. 41 Chekhova street, Rostov-on-Don 344090, Russia

[‡]zhidel@sfnedu.ru

Received 15 April 2021; Accepted 14 May 2021; Published 11 June 2021

In this paper, we report the successful growth of 0.5BiFeO₃–0.5PbFe_{0.5}Nb_{0.5}O₃/SrTiO₃/Si(001) heterostructure using RF-cathode sputtering in an oxygen atmosphere. The deposited films have been investigated by X-ray diffractometry and spectroscopic ellipsometry (SE). 0.5BiFeO₃–0.5PbFe_{0.5}Nb_{0.5}O₃ films on silicon substrates with a strontium titanate buffer layer are single-phase, polycrystalline with a texture in the 001 direction. The unit cell parameters calculated in the tetragonal approximation were $c = 4.005 \pm 0.001 \text{ \AA}$; $a = 3.995 \pm 0.001 \text{ \AA}$. The presence in the films of small unit cell deformation arising from different unit cells parameters of the film and substrate is observed. Dielectric properties and capacitance-voltage characteristics have been measured. The ellipsometric parameters have been obtained.

Keywords: Relaxation non-Debye type process; phase transition; high-temperature multiferroic; polycrystalline thin films.

1. Introduction

In the last decade, in physical materials science, considerable attention has been paid to obtaining and studying the regularities of the properties formation in high-temperature multiferroics.¹ Since both ferroelectric (FE) and magnetic properties are simultaneously manifested in them. This is due to the rather large prospects for their use in the form of ceramics or thin films as elements of various sensors and detectors, and also due to the great interest from a fundamental point of view.

Much attention is given to individual compounds (BiFeO₃, BiMnO₃, SrFe_{2/3}W_{1/3}O₃) made in the form of powders, ceramics, single crystals, and thin films, as well as composites with their participation. As can be seen from the literature analysis, bismuth ferrite (BiFeO₃, BFO) is one of the most well-known and promising multiferroics with a perovskite-type structure. This is owing to the high temperatures of both the FE-paraelectric phase transition ($T_C \sim 1103 \text{ K}$) and the magnetic one (the phase transition from the paramagnetic to the antiferromagnetic G-type phase with cycloidal magnetic ordering in the direction [110] with a period of 620 \AA occurs at $T_N \sim 643 \text{ K}$).^{2,3} The crystal structure of BiFeO₃ is rhombohedral (space group $R3c$).⁴ The spontaneous polarization reaches $100 \mu\text{C}/\text{cm}^2$. Magnetoelectric interactions directly are

rather weak in BiFeO₃ (the magnetoelectric coefficient (α_{ME}) is less than $2.5 \text{ mV}/(\text{cm} \cdot \text{Oe})$ in ceramics).⁵ This is due to the high temperatures of the magnetic and structural ordering, the significant difference between them, and the thermodynamic instability of BiFeO₃. It should be pointed out that BFO is at the limit of stability of the structural type of perovskite both in the directionality parameter and in the chemical bond strength parameter.⁶ In addition, the boundary position of bismuth ferrite, along with the presence of bismuth and iron cations in its composition, whose valence can change during synthesis, contributes to the formation and accumulation of defects. One can include oxygen vacancies, since they define the high level of total electrical conductivity of ceramics and its low electrical strength. All this imposes significant restrictions on the use of bismuth ferrite to manufacture multifunctional devices. Creating solid solutions based on bismuth ferrite, such as Bi_{1-x}Ln_xFeO₃ (Ln – rare earth ion), Bi_{1-x}A_xFeO₃ (A – alkaline earth ion), BiFe_{1-x}Ti_xO_{3+δ} with improved magnetic, electrical, and magnetoelectric properties is a chance of solving these problems.

This paper presents the results obtained from investigation of ceramics and thin films of a solid solution with the composition 0.5BiFeO₃–0.5PbFe_{0.5}Nb_{0.5}O₃ (0.5BFO–0.5PFN), in which multiferroic (lead ferroniobate with $T_C \sim 370 \text{ K}$ and $T_N \sim 393\text{--}433 \text{ K}$) was chosen as the second component.

[‡]Corresponding author.

2. Experimental Procedures

The solid solution of the $0.5\text{BiFeO}_3\text{--}0.5\text{PbFe}_{0.5}\text{Nb}_{0.5}\text{O}_3$ stoichiometric composition was the object of study. The samples were synthesized by solid-phase reactions using Bi_2O_3 , PbO , Fe_2O_3 , and Nb_2O_5 oxides. Sintering was carried out using conventional ceramic technology. Material synthesis procedure is presented in Ref. 6.

The structural perfection of the films, the unit cell parameters in the direction normal to the substrate plane, and the orientation relations between the film and the substrate were established by X-ray diffraction with $\theta/2\theta$ method using DRON-4-07 diffractometer ($\text{Cu}_{K\alpha}$ -radiation). X-ray diffraction patterns confirmed the formation of pure ceramic samples. The $0.5\text{BFO--}0.5\text{PFN}$ solid solution has a pseudocubic structure at room temperature with the cell parameter $a = 3.999(5)$ Å.

The $0.5\text{BiFeO}_3\text{--}0.5\text{PbFe}_{0.5}\text{Nb}_{0.5}\text{O}_3/\text{SrTiO}_3/\text{Si}(001)$ heterostructures were created by high-frequency sputtering of ceramic targets of the corresponding composition in the high-current γ -discharge mode at oxygen pressures of 0.43 Torr. Monocrystalline p -type silicon with resistivity of $12 \Omega \cdot \text{cm}$ (KDB12), (001) cut and 0.35 mm thick (produced by MTI Corporation, USA) was used as a substrate.

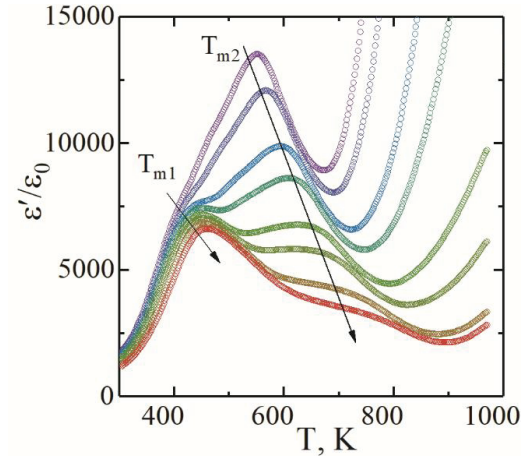
The capacitance-voltage characteristics ($C(U)$ dependences) were measured using TF Analyzer 2000 equipped with an FE module. The frequency was 100 kHz and 40 mV in amplitude. To conduct dielectric measurements of film structures, electrodes were deposited onto the entire free surface substrate and onto the film through a mask (with selected arrangement topology) with holes $\sim 180\text{--}200 \mu\text{m}$ in diameter by thermal evaporation of Al with a Cr sublayer in vacuum.

Measurements of the relative complex permittivity $\varepsilon^*/\varepsilon_0 = \varepsilon'/\varepsilon_0 - i\varepsilon''/\varepsilon_0$ (ε' and ε'' are the real and imaginary parts of ε^* , respectively, ε_0 is the dielectric constant) were conducted in the frequency range $f = 20\text{--}2 \cdot 10^6$ Hz at $T = (10\text{--}300)$ K. To examine relative complex permittivity in the temperature range $T = (300\text{--}1000)$ K the LCR automatic test system based on Agilent E4980A and Varta TP703 thermostat were used.

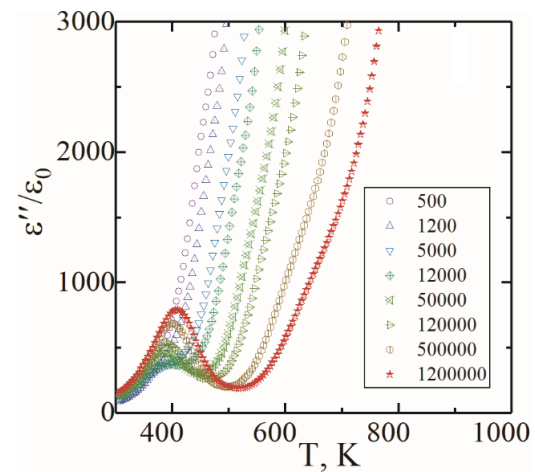
Spectroscopic ellipsometry (SE) measurements have been performed on a spectral complex (ELLIPS-1991) based on a static measuring circuit in the wavelength range of 350–1000 nm in the SSC RAS Center of Collective Use (No. 501994). SE measurements have been carried out with a step of 2 nm and at an incidence angle of 65° . To avoid problems related to surface nonuniformities, the fitting was realized in the spectral range 400–1000 nm using the “Spectroscan” software package.

3. Experimental Results and Discussion

Figure 1 shows $\varepsilon'/\varepsilon_0(T, f)$ and $\varepsilon''/\varepsilon_0(T, f)$ dependences for $0.5\text{BiFeO}_3\text{--}0.5\text{PbFe}_{0.5}\text{Nb}_{0.5}\text{O}_3$ ceramics. The presence of two relaxing (frequency-dependent) maxima at T_{m1} and T_{m2} is a specific feature of the $\varepsilon'/\varepsilon_0(T, f)$ dependences. The first



(a)



(b)

Fig. 1. (a) $\varepsilon'/\varepsilon_0(T, f)$ and (b) $\varepsilon''/\varepsilon_0(T, f)$ dependences for $0.5\text{BiFeO}_3\text{--}0.5\text{PbFe}_{0.5}\text{Nb}_{0.5}\text{O}_3$ ceramics.

maximum $\varepsilon'/\varepsilon_0(T, f)$ and the preceding maximum $\varepsilon''/\varepsilon_0(T, f)$ are typical for relaxors. Namely, with increasing frequency and temperature the height of relaxing $\varepsilon'/\varepsilon_0(T, f)$ maxima decreases, and the height of $\varepsilon''/\varepsilon_0(T, f)$ maxima increases.

A characteristic feature of the $\varepsilon''/\varepsilon_0(T)$ dependences at $T > T_{m1}$ is the rapid growth of $\varepsilon''/\varepsilon_0$ at temperatures that increase with an increase in the frequency of the measuring field. This is caused by an increase in the through conduction (most likely, grain volume), which makes a significant contribution to $\varepsilon''/\varepsilon_0$. The consequence of the increase in conductivity is the absence of $\varepsilon''/\varepsilon_0(T)$ maxima at $T = T_{m1}$ at low frequencies, and only the formation of “humps.” The $\varepsilon'/\varepsilon_0(T)$ maxima at T_{m2} , in comparison with the maxima at $T = T_{m1}$, are more diffuse, and the corresponding maximum $\varepsilon''/\varepsilon_0(T, f)$ becomes hardly noticeable in the low-frequency region due to an increase in this temperature range through electrical conductivity of ceramics, as will be shown below. For a more detailed analysis of the dielectric spectra, the $\varepsilon'/\varepsilon_0(f)$, $\varepsilon''/\varepsilon_0(f)$, $\gamma'(f)$, and $\varepsilon''/\varepsilon_0(\varepsilon'/\varepsilon_0)$ dependences (Fig. 2) were studied.

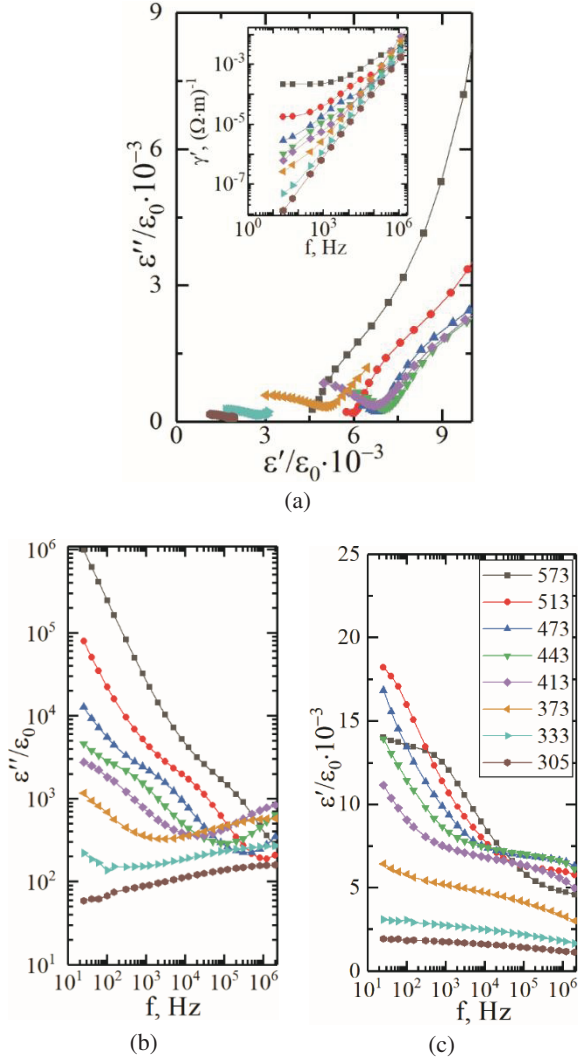


Fig. 2. (a) $\epsilon''/\epsilon_0(\epsilon'/\epsilon_0)$, $\gamma'(f)$ (insert); (b) $\epsilon''/\epsilon_0(f)$; (c) $\epsilon'/\epsilon_0(f)$ dependences of $0.5\text{BiFeO}_3\text{-}0.5\text{PbFe}_{0.5}\text{Nb}_{0.5}\text{O}_3$ ceramics for temperatures 305 K, 333 K, 373 K, 413 K, 443 K, 473 K, 513 K and 573 K.

It can be claimed from the Cole–Cole diagrams form and the nature of their change with temperature that we fix the response from two frequency-separated relaxation non-Debye type processes in the frequency range $f = 20\text{--}2 \cdot 10^6$ Hz. The first process prevails at temperatures below 423 K, and the second — more than 573 K, and they coexist in the temperature range 423–573 K. The $\gamma'(f)$ dependence (Fig. 2(a), insert) reaches a plateau at low frequencies only at $T > 473$ K.

This indicates that it is necessary to take into account the contribution of the singular term $\gamma'_{\omega \rightarrow 0}/(\epsilon_0 \cdot f)$, determined by the contribution of the through conduction,⁷ when approximating dependences (see Eq. (1)):

$$\epsilon^* = \epsilon_{\infty 1} + \frac{\epsilon_{s1} - \epsilon_{\infty 1}}{1 + (i\omega\tau_1)^{1-\alpha_1}} + \frac{\epsilon_{s2} - \epsilon_{s1}}{1 + (i\omega\tau_2)^{1-\alpha_2}} + i \frac{\gamma_{st}}{\omega\epsilon_0}, \quad (1)$$

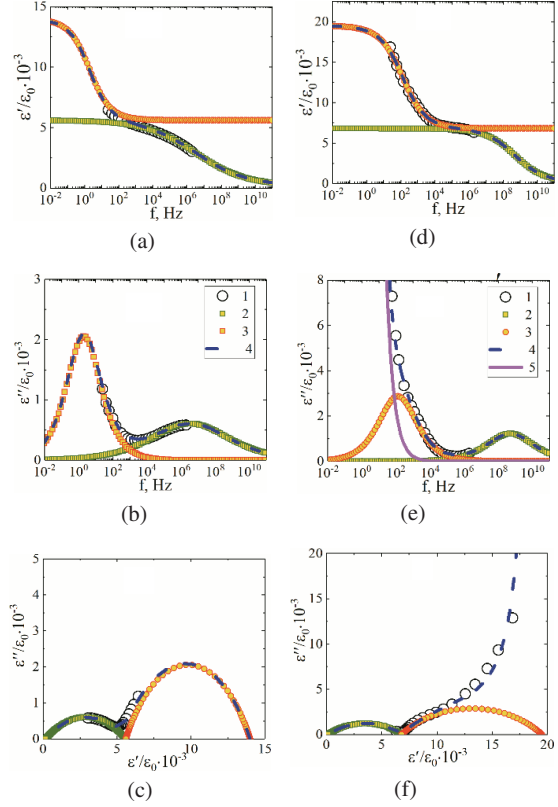


Fig. 3. Experimental and theoretical $\epsilon'/\epsilon_0(f)$, $\epsilon''/\epsilon_0(f)$, $\epsilon''/\epsilon_0(\epsilon'/\epsilon_0)$ curves of $0.5\text{BiFeO}_3\text{-}0.5\text{PbFe}_{0.5}\text{Nb}_{0.5}\text{O}_3$ ceramics for temperatures 373 K (a)–(c) and 473 K (d)–(f). On graphs: 1 – experimental results; 2 – approximation from the contribution of the first process to Eq. (1); 3 – approximation from the contribution of the second process to Eq. (1); 4 – approximation according to Eq. (1); 5 – the contribution of the singular term to Eq. (1).

where ϵ_{s1} , ϵ_{s2} and $\epsilon_{\infty 1}$ are static and high-frequency permeabilities; τ_1 and τ_2 are relaxation times; α_1 and α_2 are the relaxation time distribution coefficients (from 0 to 1); γ_{st} is the electrical conductivity of ceramics at $f \rightarrow 0$.

One can clearly see the digestibility of using Eq. (1) from the approximation results. As an example, Fig. 3 shows the approximation results for individual temperatures.

Thus, one can argue that significant changes in the real structure of the material occur when temperature is measured in the $0.5\text{BiFeO}_3\text{-}0.5\text{PbFe}_{0.5}\text{Nb}_{0.5}\text{O}_3$ multiferroic ceramic (phase transitions in both FE and magnetic subsystem) taking into account the results obtained and information from Ref. 8. In this case, the effects of interlayer polarization and the corresponding non-Debye dielectric relaxation begin to manifest themselves in the paraelectric phase due to an increase in the electrical conductivity of the material. A consequence of this dielectric relaxation is a sharp increase in the ϵ'/ϵ_0 values in the paraelectric region, reaching values of more than 15,000. At room temperature, the dispersion of dielectric parameters in the material was weak, and the ϵ'/ϵ_0 values were $\sim 1700\text{--}2000$ at ϵ''/ϵ_0 values less than 200. These parameters were account for analyzing the parameters of

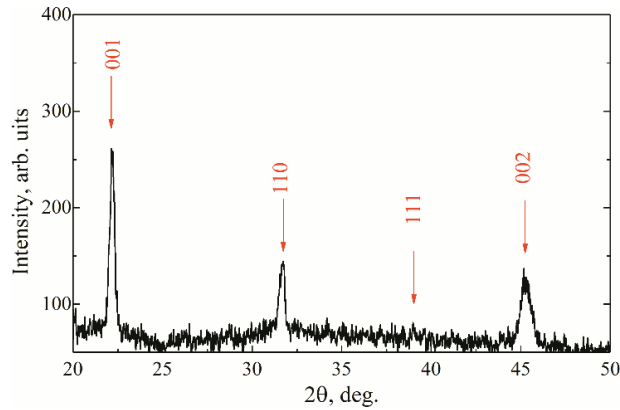


Fig. 4. XRD pattern of $0.5\text{BiFeO}_3\text{-}0.5\text{PbFe}_{0.5}\text{Nb}_{0.5}\text{O}_3/\text{SrTiO}_3/\text{Si}(001)$ heterostructure.

polycrystalline $0.5\text{BiFeO}_3\text{-}0.5\text{PbFe}_{0.5}\text{Nb}_{0.5}\text{O}_3$ multiferroic thin films.

In Fig. 4, X-ray diffraction pattern of $0.5\text{BiFeO}_3\text{-}0.5\text{PbFe}_{0.5}\text{Nb}_{0.5}\text{O}_3/\text{SrTiO}_3/\text{Si}(001)$ is presented.

It should be noted that we succeeded in obtaining $0.5\text{BiFeO}_3\text{-}0.5\text{PbFe}_{0.5}\text{Nb}_{0.5}\text{O}_3$ films on silicon substrates only when using a strontium titanate buffer layer by analogy with Ref. 9, as we did in preparing PZT films. It can be seen that the films obtained are single-phase, polycrystalline with a texture in the 001 direction. The unit cell parameters calculated in the tetragonal approximation were $c = 4.005 \pm 0.001 \text{ \AA}$; $a = 3.995 \pm 0.001 \text{ \AA}$. This indicates the presence in the films of small unit cell deformation arising from different unit cells parameters of the film and substrate (in ceramics $a = c = 3.999(5) \text{ \AA}$ ⁶). No foreign phases in the form of simple oxides, including oxides based on silicon, have been detected by X-ray diffractometry in the test samples. It means that the used SrTiO_3 thin layer in the heterostructure preparation: (1) is “orienting” for the perovskite phase growth

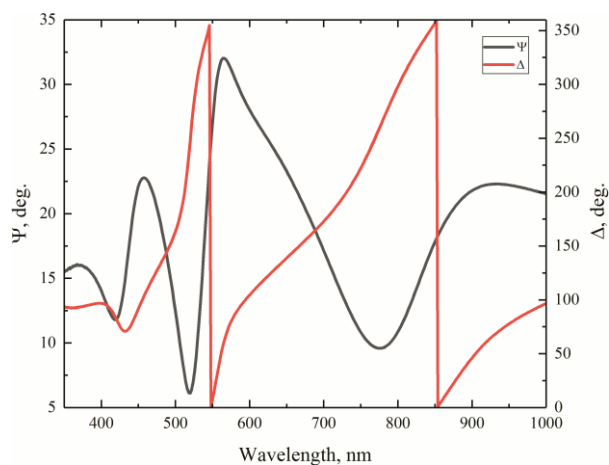


Fig. 5. Angle dependence of ellipsometric Δ and Ψ for $0.5\text{BiFeO}_3\text{-}0.5\text{PbFe}_{0.5}\text{Nb}_{0.5}\text{O}_3/\text{SrTiO}_3/\text{Si}(001)$ heterostructure.

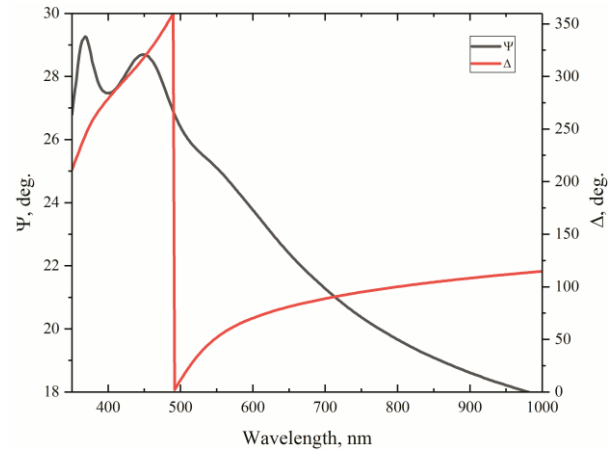


Fig. 6. Angle dependence of ellipsometric Δ and Ψ for SrTiO_3 layer on $\text{Si}(001)$ substrate.

(apparently, the phase with pyrochlore-type structure is more energetically favorable for direct heteroepitaxial growth of this class materials on the Si surface); (2) is a buffer layer, in which the relaxation arising during film synthesis occurs, and, as a result, the deformation values fixed in the film are quite small.

Figure 5 shows the results of studying the $0.5\text{BiFeO}_3\text{-}0.5\text{PbFe}_{0.5}\text{Nb}_{0.5}\text{O}_3/\text{SrTiO}_3/\text{Si}(001)$ heterostructure on spectral ellipsometer in the range 300–1000 nm.

The obtained ellipsometric parameters Δ and Ψ for the SrTiO_3 films deposited on $\text{Si}(001)$ substrates are shown in Fig. 6.

The optical model used for fitting (Fig. 7) takes into consideration a heterostructure composed of the substrate, SiO_2 and SrTiO_3 layers, and the $0.5\text{BFO}\text{-}0.5\text{PFN}$ thin film.

It is possible to achieve a good agreement with the experimental data on the spectral characteristics ψ and Δ , and to determine the optical parameters of the layers using the model selected. The constructed optical model of the film well describes the experimental spectra. The possibility of simultaneous determination of the individual nanolayers thicknesses and their complex refractive indices will be demonstrated in future works.

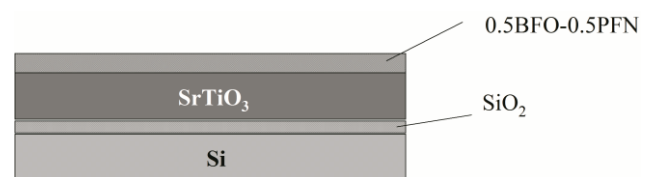


Fig. 7. Optical model used for fitting experimental angle dependence of ellipsometric Δ and Ψ for studied heterostructure.

4. Conclusions

In conclusion, we have presented results regarding the synthesis and properties of $0.5\text{BiFeO}_3\text{-}0.5\text{PbFe}_{0.5}\text{Nb}_{0.5}\text{O}_3$ ceramics and polycrystalline films. High-frequency sputtering in an oxygen atmosphere from $0.5\text{BiFeO}_3\text{-}0.5\text{PbFe}_{0.5}\text{Nb}_{0.5}\text{O}_3$ ceramic targets on monocrystalline *p*-type silicon substrates resulted into polycrystalline films with a texture in the 001 direction. XRD studies confirmed the formation of single-phase films. The unit cell parameters calculated for films in the tetragonal approximation were $c = 4.005 \pm 0.001$ Å; $a = 3.995 \pm 0.001$ Å. Meanwhile, the $0.5\text{BFO}\text{-}0.5\text{PFN}$ solid solution has a pseudocubic structure at room temperature with the cell parameter $a = 3.999(5)$ Å. It indicates the presence in the films of small unit cell deformation arising from different unit cells parameters of the film and substrate. The presence of contributions to the dielectric response from two relaxation processes was revealed in ceramics at $T > 300$ K. They contribute to the dielectric response of ceramics, each one is of a non-Debye type. Spectra of ellipsometric parameters have been obtained from SE measurements in the range 300–1000 nm. In further works, we plan to define the refractive index and extinction coefficient for this polycrystalline thin films.

Acknowledgments

The study was carried out with the financial support of the Ministry of Science and Higher Education of the Russian Federation (State task in the field of scientific activity, scientific project No. (0852-2020-0032)/(BAZ0110/20-3-07IF)).

References

- ¹ A. P. Pyatakov and A. K. Zvezdin, Magnetolectric and multiferroic media, *Phys.-Usp.* **55**, 557 (2012).
- ² Yu. N. Venevtsev, V. V. Gagulin and V. N. Lyubimov, *Ferroelectromagnets* (Nauka, Moscow, 1982).
- ³ A. M. Kadomtseva, Yu. F. Popov, A. P. Pyatakov, G. P. Vorob'ev, A. K. Zvezdin and D. Viehland, Phase transitions in multiferroic BiFeO_3 crystals, thin-layers, and ceramics: enduring potential for a single phase, room-temperature magnetolectric “holy grail”, *Phase Transit.* **79**, 1019 (2006).
- ⁴ D. Bochenek, P. Niemiec, P. Guzdek and M. Wzorek, Magnetolectric and electric measurements of the $(1-x)\text{BiFeO}_3\text{-}(x)\text{-Pb}(\text{Fe}_{1/2}\text{Nb}_{1/2})\text{O}_3$ solid solutions, *Mater. Chem. Phys.* **195**, 199 (2017).
- ⁵ E. G. Fesenko, *Perovskite Family and Ferroelectricity* (Atomizdat, Moscow, 1972).
- ⁶ L. A. Shilkina, A. V. Pavlenko, L. A. Reznitchenko, I. A. Verbenko, Phase diagram of the system of $(1-x)\text{BiFeO}_3\text{-}x\text{PbFe}_{0.5}\text{Nb}_{0.5}\text{O}_3$ solid solutions at room temperature, *Crystallogr. Rep.* **61**, 263 (2016).
- ⁷ A. S. Bogatin and A. V. Turik, *Relaxation Polarization Processes in Dielectrics with High Through Conduction* (Feniks, Rostov-on-don, 2013).
- ⁸ A. V. Pavlenko, K. M. Zhidel and L. A. Shilkina, $0.5\text{BiFeO}_3\text{-}0.5\text{PbFe}_{0.5}\text{Nb}_{0.5}\text{O}_3$ multiferroic ceramic: Structure, dielectric and magnetodielectric properties, *Phys. Solid State.* **62**, 1880 (2020).
- ⁹ S. P. Zinchenko, D. V. Stryukov, A. V. Pavlenko and V. M. Mukhortov, The effect of a $\text{Ba}_{0.2}\text{Sr}_{0.8}\text{TiO}_3$ sublayer on the structure and electric characteristics of lead zirconate titanate films on the Si(001) substrate, *Tech. Phys. Lett.* **46**, 1196 (2020).